ROTROCRAFT FLIGHT DYNAMICS MODEL IDENTIFICATION RESEARCH AT NUAA

Wu Wei, Nanjing University of Aeronautics and Astronautics, Nanjing, China
Chen Renliang, Nanjing University of Aeronautics and Astronautics, Nanjing, China

Abstract

The system identification is a powerful tool for high fidelity flight dynamics modeling of flying vehicles. The research in this area at Nanjing University of Aeronautics and Astronautics during the past decade is presented. Four different kinds of identification methods both in time domain and frequency domain are discussed. The time domain technique is used to identify low order models with 6 degrees of freedom, and the frequency domain method is developed to identify high order models with 9 degrees of freedom. The conventional statistic identification technique and modern deterministic identification methods are developed for different purpose. The applications of these methods to both manned helicopters and unmanned air vehicles are introduced, and the linear flight dynamics models of helicopters as well as tilt-rotor aircraft are identified successfully.

Nomenclature

$\boldsymbol{y}$	model output vector
$\boldsymbol{x}$	model input vector
$\boldsymbol{\theta}$	vector of parameters to be identified
$\boldsymbol{\varepsilon}$	bounded noise vector
$\boldsymbol{P}$	covariance matrix of $\boldsymbol{x}$
$\boldsymbol{\sigma}$	noise bound vector
$\boldsymbol{H}$	Hessian matrix
t	time variable
λ	weighting coefficient in Optimal Bounding Ellipsoid algorithm
$\boldsymbol{X}$	state variable vector of helicopter flight dynamics model
$\boldsymbol{U}$	control input vector of helicopter flight dynamics model
$\boldsymbol{Y}$	output vector of helicopter flight dynamics model
$\boldsymbol{A}$	stability matrix of helicopter flight dynamics model
$\boldsymbol{B}$	control matrix of helicopter flight dynamics model
$\boldsymbol{C}$	nonlinear terms of helicopter flight dynamics model
$\boldsymbol{D}$	observation matrix of helicopter flight dynamics model
X, Y, Z	forces along x, y, z coordinate at center of gravity of helicopters
L, M, N	roll, pitch, yaw moment at center of gravity of helicopters
u, v, w	linear velocities of helicopter in body axis
p, q, r	angular rates of helicopter in body axis
δlon	longitudinal stick input
δlat	lateral stick input
δcol	collective stick input
δped	pedal input
$\beta_0, \beta_{1c}, \beta_{1s}$	coning angle, longitudinal flapping angle and lateral flapping angle of a rotor
N	the numbers of sampling data
Ω	the rotation speed of a rotor

1. INTRODUCTION

The rotorcraft flight dynamics modeling is a very complex problem, and this is because the aerodynamic phenomenon of a rotorcraft is very complicated, the rotorcraft is unstable and it is coupled heavily. The conventional theoretical modeling technique usually makes a lot of assumptions to build the mathematic model of a rotorcraft by applying basic physical laws. However, these assumptions and approximations decrease the accuracy of the model. In order to solve this problem, the system identification technique has been applied to rotorcraft flight dynamics modeling since 1960s, and it has been proven that this kind of modeling technique can increase the accuracy as well as confidence of the flight dynamics model considerably [1-3].

During the past 10 years, in order to provide high fidelity flight dynamics model for flying quality design and flight control system design of different types of rotorcraft, a series of research in system identification have been taken out at the Nanjing University of Aeronautics and Astronautics (NUAA). Basically, there are 4 different identification methods developed in the research, e.g. multi-step identification [4], fast frequency domain identification [5-6], subspace identification [7-8], and set-membership identification [9-10]. This paper gives an overview of these identification methods as well as the applications to both manned helicopters and UAVs.

2. MULTI-STEP IDENTIFICATION

The time domain identification is a direct and easy-to-implement method for rotorcraft flight dynamics modeling. In NUAA, the time domain identification is used to identify the rotorcraft linear flight dynamics model with the degrees of freedom ranges from three to six. Generally, the multi-step method, the subspace method and the set-membership method are all belong to time domain identification. In this section, only the multi-step method will be introduced and the latter two methods will be discussed in later sections.

The conventional time domain identification method usually requires model structure identification before final parameter identification. However, the structure identification procedure is quite time consuming in time domain. In order to solve this problem, a multi-step identification method which does not require model structure identification is developed in NUAA to increase the identification efficiency.

2.1. Identification Model

The multi-step identification method is used to identify the following 6 degrees of freedom rigid body flight dynamics model in time domain.

(1) $$\dot{\boldsymbol{x}} = \boldsymbol{A}\boldsymbol{x} + \boldsymbol{B}\boldsymbol{u} + \boldsymbol{C}$$

in which,

$\boldsymbol{x} = [\Delta u, \Delta v, \Delta w, \Delta p, \Delta q, \Delta r]^T$, represents the state vector of the rotorcraft.

$\boldsymbol{u} = [\Delta\delta_{long}, \Delta\delta_{lat}, \Delta\delta_{col}, \Delta\delta_{ped}]^T$, represents the control input vector.

$\boldsymbol{A}$ is the stability derivative matrix, $\boldsymbol{B}$ is the control derivative matrix, and $\boldsymbol{C}$ is the nonlinear terms of gravity and inertial forces.

The Eq. (1) is a semi-linear equation, and it has been proven that this kind of flight dynamics model will increase the numeric stability in time domain identification. This is because, in time domain, it always need integrate Eq. (1) to obtain state vector. However, the small error in the single integration step will be cumulated, and it may lead to a failure of the identification caused by large integration error. So the exclusion of 3 Euler angle equations (which do not have any parameters to be identified) and keep the nonlinearity of gravity as well as inertial forces will help decreasing the integration error and increasing the numeric stability of the identification.

2.2. Identification Algorithm

The procedure of multi-step identification can be divided into several steps. In the first step, single channel dynamics models as shown in Eq. (2) ~ Eq. (5) are used. There are only the most sensitive parameters such as pitch and roll damping etc. in these equations, so the ill-conditioned problem of information matrix will be avoided in identifying such models.

(2) $$\begin{bmatrix}\Delta\dot{u}\\ \Delta\dot{q}\end{bmatrix} = \begin{bmatrix}X_u & X_q\\ M_u & M_q\end{bmatrix}\bullet\begin{bmatrix}\Delta u\\ \Delta q\end{bmatrix} + \begin{bmatrix}X_{\delta long}\\ M_{\delta long}\end{bmatrix}\bullet\Delta\delta_{long} + \begin{bmatrix}-g\sin\theta + rv - qw + a_{x0}\\ \dot{q}_0\end{bmatrix}$$

(3) $$\begin{bmatrix}\Delta\dot{v}\\ \Delta\dot{p}\end{bmatrix} = \begin{bmatrix}Y_v & Y_p\\ L_v & L_p\end{bmatrix}\bullet\begin{bmatrix}\Delta v\\ \Delta p\end{bmatrix} + \begin{bmatrix}Y_{\delta lat}\\ L_{\delta lat}\end{bmatrix}\bullet\Delta\delta_{lat} + \begin{bmatrix}g\cos\theta\sin\varphi + pw - ru + a_{y0}\\ \dot{p}_0\end{bmatrix}$$

(4) $$\Delta\dot{w} = Z_w\bullet\Delta w + Z_{\delta col}\bullet\Delta\delta_{col} + g\cos\theta\cos\varphi + qu - pv + a_{z0}$$

(5) $$\Delta\dot{r} = N_r\bullet\Delta r + N_{\delta ped}\bullet\Delta\delta_{ped} + \dot{r}_0$$

The least square method is applied to Eq. (2) ~ Eq. (5) to obtain the estimation of all derivatives. Then in the second step, a more powerful estimator e.g. maximum likelihood method is used as shown in Eq. (6) ~ Eq. (8) to refine the identification results obtained in step 1.

(6) $$\boldsymbol{\theta}^{t+1} = \boldsymbol{\theta}^t - \left(\frac{\partial^2 J}{\partial\boldsymbol{\theta}^2}\right)^{-1}\bullet\frac{\partial J}{\partial\boldsymbol{\theta}}$$

(7) $$\left(\frac{\partial^2 J}{\partial\boldsymbol{\theta}^2}\right)_{ij} = \frac{2}{N}\sum_{n=1}^{N}\left(\frac{\partial\boldsymbol{v}}{\partial\theta_i}\right)^T\bullet\boldsymbol{R}^{-1}\frac{\partial\boldsymbol{v}}{\partial\theta_j}$$

(8) $$\left(\frac{\partial J}{\partial\boldsymbol{\theta}}\right)_i = \frac{2}{N}\sum_{n=1}^{N}\boldsymbol{v}\bullet\boldsymbol{R}^{-1}\frac{\partial\boldsymbol{v}}{\partial\theta_i}$$

The sensitivity function of prediction error in Eq. (7) and Eq. (8) can be obtained by solving Eq. (9).

(9) $$\frac{d}{dt}\left(\frac{\partial\boldsymbol{x}}{\partial\theta_i}\right) = \boldsymbol{A}\frac{\partial\boldsymbol{x}}{\partial\theta_i} + \frac{\partial\boldsymbol{A}}{\partial\theta_i}\boldsymbol{x} + \frac{\partial\boldsymbol{B}}{\partial\theta_i}\boldsymbol{u}$$

The main derivatives in each channel will have a good estimation that close to the true value after step 2. So in the third step, weak coupled models as shown in Eq. (10) and Eq. (11) will be used to identify more parameters and refine the values of main derivatives.

(10) $$\begin{bmatrix}\Delta\dot{u}\\ \Delta\dot{w}\\ \Delta\dot{q}\end{bmatrix} = \begin{bmatrix}X_u & X_w & X_q\\ Z_u & Z_w & Z_q\\ M_u & M_w & M_q\end{bmatrix}\bullet\begin{bmatrix}\Delta u\\ \Delta w\\ \Delta q\end{bmatrix} + \begin{bmatrix}X_{\delta long} & X_{\delta col}\\ Z_{\delta long} & Z_{\delta col}\\ M_{\delta long} & M_{\delta col}\end{bmatrix}\bullet\begin{bmatrix}\Delta\delta_{long}\\ \Delta\delta_{col}\end{bmatrix} + \begin{bmatrix}-g\sin\theta + rv - qw + a_{x0}\\ g\cos\theta\cos\varphi + qu - pv + a_{z0}\\ \dot{q}_0\end{bmatrix}$$

(11) $$\begin{bmatrix}\Delta\dot{v}\\ \Delta\dot{p}\\ \Delta\dot{r}\end{bmatrix} = \begin{bmatrix}Y_v & Y_p & Y_r\\ L_v & L_p & L_r\\ N_v & N_p & N_r\end{bmatrix}\bullet\begin{bmatrix}\Delta v\\ \Delta p\\ \Delta r\end{bmatrix} + \begin{bmatrix}Y_{\delta lat} & Y_{\delta ped}\\ L_{\delta lat} & L_{\delta ped}\\ N_{\delta lat} & N_{\delta ped}\end{bmatrix}\bullet\begin{bmatrix}\Delta\delta_{lat}\\ \Delta\delta_{ped}\end{bmatrix} + \begin{bmatrix}g\cos\theta\sin\varphi + pw - ru + a_{y0}\\ \dot{p}_0\\ \dot{r}_0\end{bmatrix}$$

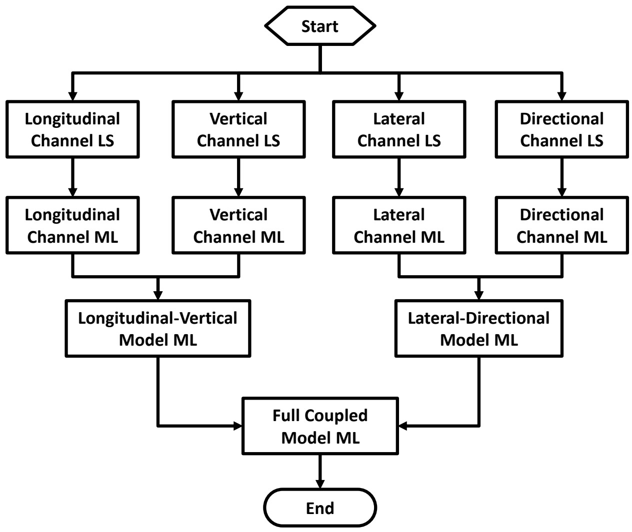

Fig. 1 Flowchart for Multi-step Identification Method

The maximum likelihood algorithm is used to identify the above models, and two groups of flight test data with different excitation input are used for each model in this step. Finally, in the fourth step, the full coupled model as shown in Eq. (1) is used, and since the main derivatives in the model have almost converged already, the sensitivity matrix will not be ill-conditioned. So a maximum likelihood algorithm can be used directly to identify the final model.

In summary, the multi-step identification method can be illustrated in Fig. 1. Where, “LS” is short for Least Square and “ML” represents Maximum Likelihood.

3. FAST FREQUENCY DOMAIN IDENTIFICATION

The rotorcraft is a typical high order system, for some applications such as simulation model validation, high bandwidth flight control system design etc., a high order model is required. In the past few years, in order to provide high fidelity flight dynamics model for flying quality analysis and flight control system design of helicopters, the NUAA worked together with the China helicopter industry to carry out some research on the identification of flight dynamics model with rotor degrees of freedom. Because there are much more parameters to be identified in a high model relative to a rigid body model, the time domain identification becomes very inefficient. On the other hand, the time domain method always gives higher weightings to low frequency derivatives during identification, which lead to poor estimation of high frequency parameters such as rotor derivatives etc. In order to solve these problems, a frequency domain identification method has been developed. In this section, some details of the developed method including the high order identification model, the frequency domain identification strategy as well as the acceleration algorithm will be discussed.

3.1. High Order Identification Model

In order to build a high order flight dynamics model of a rotorcraft, the rotor dynamics model is required. In our research, the rotor dynamics model only contains the flapping degrees of freedom, and the lagging of a blade is neglected. Generally, there are two different rotor flapping dynamics models used. The first one is established based on a simplified theoretical flapping model and it is used to identify the flight dynamics model of model-scaled rotorcraft. This kind of high order model is simple and will be introduced in the next section. The second one is developed to identify a manned helicopter. This flapping model is established without using any theoretical models, and it is fully parameterized which is quite suitable for identification purpose.

Assuming the rotorcraft is in stable flight, which is always true during the flight test for identification purpose. Then a steady flapping is existed, the relationship between the rotor flapping angle and the single blade flapping angle can be expressed as Eq. (12) ~ Eq. (14).

(12) $$\beta_0 = \frac{1}{N}\sum_{i=1}^{N}\beta_i$$

(13) $$\beta_{1c} = \frac{2}{N}\sum_{i=1}^{N}\beta_i\cos\psi_i$$

(14) $$\beta_{1s} = \frac{2}{N}\sum_{i=1}^{N}\beta_i\sin\psi_i$$

Take the first and second order time derivatives to both sides of Eq. (12) ~ Eq. (14), then after some mathematical manipulation, the rotor flapping equation can be obtained as shown in Eq. (15).

(15) $$\begin{cases} \ddot{\beta}_0 = M_{rot}^0 \\ \ddot{\beta}_{1c} = M_{rot}^{1c} + \Omega^2 \beta_{1c} - 2\Omega \dot{\beta}_{1s} \\ \ddot{\beta}_{1s} = M_{rot}^{1s} + \Omega^2 \beta_{1s} + 2\Omega \dot{\beta}_{1c} \end{cases}$$

The Eq. (15) can be linearized, and a state space form rotor flapping dynamics model is obtained as shown in Eq. (16).

(16) $$\dot{\boldsymbol{\beta}} = \boldsymbol{A}_f \boldsymbol{\beta} + \boldsymbol{F}$$

in which,

$\boldsymbol{\beta} = \left[\Delta\beta_0, \Delta\beta_{1c}, \Delta\beta_{1s}, \Delta\dot{\beta}_0, \Delta\dot{\beta}_{1c}, \Delta\dot{\beta}_{1s}\right]^T$ is the rotor flapping state vector

$\boldsymbol{F} = \left[0, 0, 0, \Delta M_{rot}^0, \Delta M_{rot}^{1c}, \Delta M_{rot}^{1s}\right]^T$ is a vector contains rotor flapping moments,

$$\boldsymbol{A}_f = \begin{bmatrix} 0 & 0 & 0 & 1 & 0 & 0 \\ 0 & 0 & 0 & 0 & 1 & 0 \\ 0 & 0 & 0 & 0 & 0 & 1 \\ 0 & 0 & 0 & 0 & 0 & 0 \\ 0 & \Omega^2 & 0 & 0 & 0 & -2\Omega \\ 0 & 0 & \Omega^2 & 0 & 2\Omega & 0 \end{bmatrix}$$

Combined the above rotor flapping dynamics model with rigid body model, a fully parameterized high order linear flight dynamics model is obtain as shown in Eq. (17)

(17) $$\dot{\boldsymbol{x}} = \boldsymbol{A}\boldsymbol{x} + \boldsymbol{B}\boldsymbol{u}$$

in which,

$\boldsymbol{x} = [\Delta u, \Delta v, \Delta w, \Delta p, \Delta q, \Delta r, \Delta\varphi, \Delta\theta, \Delta\beta_0, \Delta\beta_{1c}, \Delta\beta_{1s}, \Delta\dot{\beta}_0, \Delta\dot{\beta}_{1c}\Delta\dot{\beta}_{1s}]^T$

, and $\boldsymbol{u} = \left[\Delta\delta_{long}, \Delta\delta_{lat}, \Delta\delta_{col}, \Delta\delta_{ped}\right]^T$. The A and B matrix now have a dimension of 14×14 and 14×9 respectively.

3.2. Identification Method

The basic identification algorithm can be illustrated in Fig. 2 below.

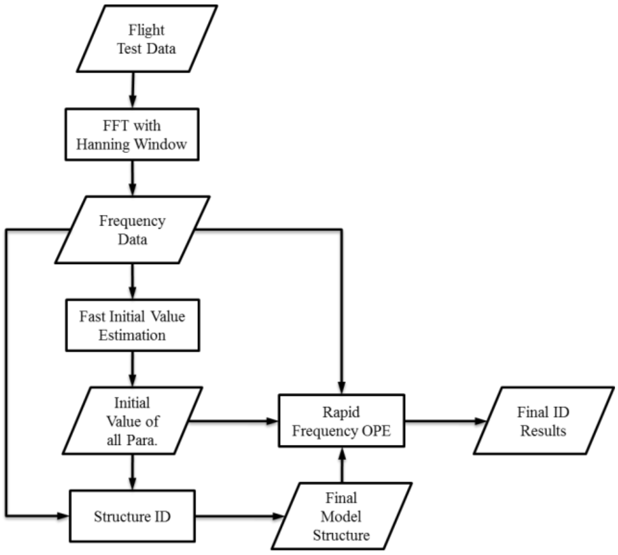

Fig. 2 Fast Frequency Domain Identification

The flight test data is transformed to frequency domain by a FFT algorithm with Hanning window. Then an initial value estimation algorithm based on frequency domain least square method, a model structure identification procedure and a rapid frequency domain output error method are applied to Eq. (17) to obtain the identification result.

- Initial Value Estimation

The aim of this procedure is to get a rough estimation of all parameters to be identified in Eq. (17). A frequency domain least square algorithm is used to finish this job. In order to do this, the Eq. (17) is transformed into frequency domain and rewrite as Eq. (18). Then the identification can be implemented using Eq. (19).

(18) $$\boldsymbol{Y}(\omega) = \boldsymbol{X}(\omega) \bullet \boldsymbol{\theta}$$

(19) $$\boldsymbol{\theta} = (\boldsymbol{X}^T \boldsymbol{X})^{-1} \boldsymbol{X}^T \boldsymbol{Y}$$

- Model Structure Identification

The model structure identification is done by using both Cramer-Rao bound and Insensitivity function. The formulas of these two criteria are shown in Eq. (20) and Eq. (21) respectively. The calculation of Cramer-Rao bound and Insensitivity function are based on Bode sensitivity function which will be talked about later. The main approach of model structure identification is to eliminate all parameters that have either large value of Cramer-Rao bound or Insensitivity function. The eliminated parameters will be fixed to constant values during the final parameter identification. There will be three possible values for these eliminated parameters, e.g. zero, prior value or initial value estimation result. A comprehensive analysis based on theoretical model is used to determine the value selection of these parameters.

(20) $IS(i) = \sqrt{(\boldsymbol{H}_{ii})^{-1}}, \quad (i = 1, 2, \cdots)$

(21) $\boldsymbol{CR}(i) = \sqrt{(\boldsymbol{H})^{-1}_{ii}}, \quad (i = 1, 2, \cdots)$

- Rapid Frequency Domain Output Error Method

The final parameter identification is implemented by a frequency domain output error method. In frequency domain, the state vector $\boldsymbol{x}$ in Eq. (17) has an analytical solution as shown in Eq. (22), and this solution can be rewrite in Bode plot form as shown in Eq. (23). Where the Re[•] and Im[•] represent the real and imaginary part of a complex variable.

(22) $$\boldsymbol{x}(\omega) = (j\omega \boldsymbol{I} - \boldsymbol{A})^{-1} \boldsymbol{B}\boldsymbol{u}(\omega)$$

(23) $$\begin{cases} \boldsymbol{x}^{amp}(\omega) = 20\log_{10} |\boldsymbol{x}(\omega)| \\ \boldsymbol{x}^{pha}(\omega) = \arctan \dfrac{\mathrm{Im}[\boldsymbol{x}(\omega)]}{\mathrm{Re}[\boldsymbol{x}(\omega)]} \end{cases}$$

The cost function for final parameter identification based on Eq. (23) is shown as Eq. (24). Where k is a weighting coefficient which used to ensure the amplitude and phase of frequency responses have the same weightings during identification. $\boldsymbol{R}$ is error covariance matrix. N is the numbers of frequency data used for identification.

(24) $$\begin{aligned} J = \frac{1}{N}\sum_{\omega=\omega_0}^{N\omega_0} \Big\{ & \left[\boldsymbol{x}^{amp}(\omega) - \boldsymbol{x}_m^{amp}(\omega)\right]^T \bullet \boldsymbol{R}_{amp}^{-1} \bullet \left[\boldsymbol{x}^{amp}(\omega) - \boldsymbol{x}_m^{amp}(\omega)\right] + \\ & k \bullet \left[\boldsymbol{x}^{pha}(\omega) - \boldsymbol{x}_m^{pha}(\omega)\right]^T \bullet \boldsymbol{R}_{pha}^{-1} \bullet \left[\boldsymbol{x}^{pha}(\omega) - \boldsymbol{x}_m^{pha}(\omega)\right] \Big\} \end{aligned}$$

The Bode sensitivity function is derived based on Eq. (22) and Eq. (23), then combined with Eq. (24), the sensitivity of cost function and the element of Hessian matrix $\boldsymbol{H}$ is obtained as Eq. (25) and Eq. (26) respectively.

(25) $$\begin{aligned} \frac{\partial J}{\partial \theta_i} = \frac{2}{N}\sum_{\omega=\omega_0}^{N\omega_0} \Bigg[& \frac{20}{\ln 10} \bullet \frac{1}{|\boldsymbol{x}(\omega)|} \bullet \left|\frac{\partial \boldsymbol{x}(\omega)}{\partial \theta_i}\right| \bullet \boldsymbol{R}_{amp}^{-1} \bullet |\boldsymbol{x}(\omega)| + \\ & k \bullet \arctan \frac{\mathrm{Im}[\partial \boldsymbol{x}(\omega)/\partial \theta_i]}{\mathrm{Re}[\partial \boldsymbol{x}(\omega)/\partial \theta_i]} \bullet \boldsymbol{R}_{pha}^{-1} \bullet \arctan \frac{\mathrm{Im}[\boldsymbol{x}(\omega)]}{\mathrm{Re}[\boldsymbol{x}(\omega)]} \Bigg] \end{aligned}$$

(26) $$\begin{aligned} \boldsymbol{H}_{ij} = \frac{\partial^2 J}{\partial \theta_i \partial \theta_j} = \frac{2}{N}\sum_{\omega=\omega_0}^{N\omega_0} \Bigg[& \left(\frac{20}{\ln 10} \bullet \frac{1}{|x(\omega)|}\right)^2 \bullet \left|\frac{\partial \boldsymbol{x}(\omega)}{\partial \theta_i}\right| \bullet \boldsymbol{R}_{amp}^{-1} \bullet \left|\frac{\partial \boldsymbol{x}(\omega)}{\partial \theta_j}\right| + \\ & k \bullet \arctan \frac{\mathrm{Im}[\partial \boldsymbol{x}(\omega)/\partial \theta_i]}{\mathrm{Re}[\partial \boldsymbol{x}(\omega)/\partial \theta_i]} \bullet \boldsymbol{R}_{pha}^{-1} \bullet \arctan \frac{\mathrm{Im}[\partial \boldsymbol{x}(\omega)/\partial \theta_j]}{\mathrm{Re}[\partial \boldsymbol{x}(\omega)/\partial \theta_j]} \Bigg] \end{aligned}$$

Take Eq. (25) and Eq. (26) into Eq. (6), the final estimation of remaining parameters in Eq. (17) is obtained.

In order to increase the identification efficiency of a high order flight dynamics model, an acceleration algorithm is developed based on the fact that the convergent speed of each parameter to be identified is different. The Fig. 3 shows the basic procedure of the accelerated frequency domain output error method.

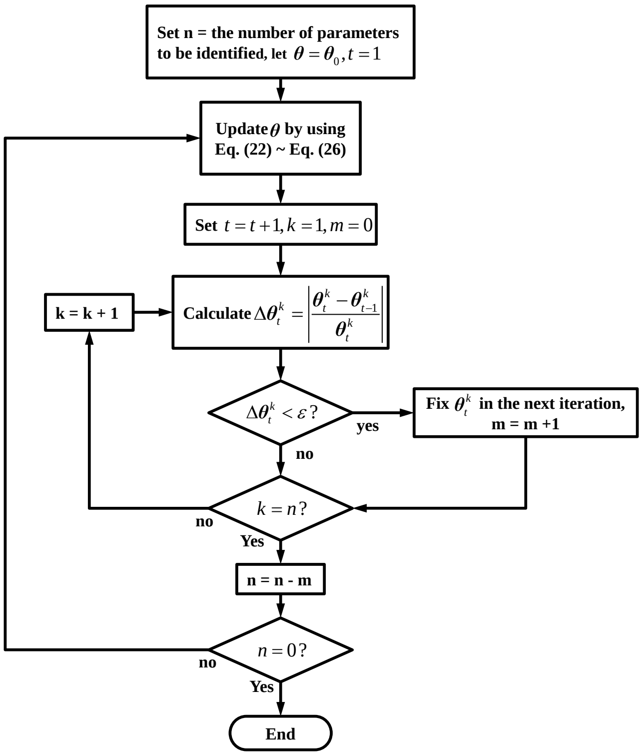

Fig. 3 Acceleration Strategy for Frequency Domain Output Error Method

4. SUBSPACE IDENTIFICATION

The conventional identification methods have some instinctive deficiencies. The detailed statistical information of measurement noise, model prediction error etc. is required in these estimators. However, it is usually difficult to obtain the above information when identifying a rotorcraft. Therefore, the accuracy and especially the robustness of the conventional identification methods are decreased. In order to solve these problems, new techniques are developed based on modern identification theory. One is the subspace identification method and the other is the set-membership identification which will be discussed in the next section.

4.1. Identification Model

The subspace identification method is used to identify model scaled rotorcraft for flight control system design. Both rigid body model and high order model are identified. When identifying the high order model for the model scaled rotorcraft, a simplified rotor flapping model as shown in Eq. (27) is used.

(27) $$\begin{cases} \tau\dot{\beta}_{1s} = -\beta_{1s} - \tau p + \beta_{1c}\tau K_\beta / 2I_\beta\Omega + A_1 \\ \tau\dot{\beta}_{1c} = -\beta_{1c} - \tau q + \beta_{1s}\tau K_\beta / 2I_\beta\Omega + B_1 \end{cases}$$

in which,

$\tau = 16/\gamma\Omega$ is the rotor time constant.

In order to apply subspace identification, the discrete flight dynamics model is required, so the differential state space equation is discretized to difference state space equation as shown in Eq. (28).

(28) $$\begin{cases} \boldsymbol{x}(t+1) = \boldsymbol{A}\boldsymbol{x}(t) + \boldsymbol{B}\boldsymbol{u}(t) \\ \boldsymbol{y}(t) = \boldsymbol{C}\boldsymbol{x}(t) + \boldsymbol{D}\boldsymbol{u}(t) + \boldsymbol{v}(t) \end{cases}$$

in which, $\boldsymbol{v}(t)$ is the measurement noise vector.

4.2. Identification Algorithm

Assuming Eq. (28) is observable and controllable, and then the following relationship is existed.

(29) $$\boldsymbol{Y}_r(t) = \boldsymbol{O}_r\boldsymbol{x}(t) + \boldsymbol{S}_r\boldsymbol{U}_r(t) + \boldsymbol{V}_r(t)$$

in which,

(30) $$\boldsymbol{Y}_r(t) = \begin{bmatrix} \boldsymbol{y}(t) & \boldsymbol{y}(t+1) & \cdots & \boldsymbol{y}(t+r-1) \end{bmatrix}^T,$$

(31) $$\boldsymbol{U}_r(t) = \begin{bmatrix} \boldsymbol{u}(t) & \boldsymbol{u}(t+1) & \cdots & \boldsymbol{u}(t+r-1) \end{bmatrix}^T,$$

(32) $$\boldsymbol{V}_r(t) = \begin{bmatrix} \boldsymbol{v}(t) & \boldsymbol{v}(t+1) & \cdots & \boldsymbol{v}(t+r-1) \end{bmatrix}^T,$$

(33) $$\boldsymbol{O}_r = \begin{bmatrix} \boldsymbol{C} & \boldsymbol{CA} & \cdots & \boldsymbol{CA}^{r-1} \end{bmatrix}^T,$$

(34) $$\boldsymbol{S}_r = \begin{bmatrix} \boldsymbol{D} & \boldsymbol{0} & \cdots & \boldsymbol{0} \\ \boldsymbol{CB} & \boldsymbol{D} & \cdots & \boldsymbol{0} \\ \vdots & \vdots & \ddots & \vdots \\ \boldsymbol{CA}^{r-2}\boldsymbol{B} & \boldsymbol{CA}^{r-3}\boldsymbol{B} & \cdots & \boldsymbol{D} \end{bmatrix}$$

If the sample time is T and takes all measurement data into Eq. (29), then Eq. (35) is obtained.

(35) $$\boldsymbol{Y} = \boldsymbol{O}_r\boldsymbol{X} + \boldsymbol{S}_r\boldsymbol{U} + \boldsymbol{V}$$

in which,

(36) $$\boldsymbol{Y} = \begin{bmatrix} \boldsymbol{Y}_r(1) & \boldsymbol{Y}_r(2) & \cdots & \boldsymbol{Y}_r(T) \end{bmatrix},$$

(37) $$\boldsymbol{X} = \begin{bmatrix} \boldsymbol{x}(1) & \boldsymbol{x}(2) & \cdots & \boldsymbol{x}(T) \end{bmatrix},$$

(38) $$\boldsymbol{U} = \begin{bmatrix} \boldsymbol{U}_r(1) & \boldsymbol{U}_r(2) & \cdots & \boldsymbol{U}_r(T) \end{bmatrix},$$

(39) $$\boldsymbol{V} = \begin{bmatrix} \boldsymbol{V}_r(1) & \boldsymbol{V}_r(2) & \cdots & \boldsymbol{V}_r(T) \end{bmatrix}$$

Let Π_u to be the orthogonal projection of matrix $\boldsymbol{U}$ which has the form:

(40) $$\Pi_u = \boldsymbol{I} - \boldsymbol{U}^H(\boldsymbol{U}\boldsymbol{U}^H)^{-1}\boldsymbol{U}$$

Multiplies the both sides of Eq. (35) by Eq. (40), and the Eq. (41) is obtained.

(41) $$\boldsymbol{Y}\Pi_u = \boldsymbol{O}_r\boldsymbol{X}\Pi_u + \boldsymbol{V}\Pi_u$$

The last term of Eq. (41) will be zero if the numbers of data is infinite. Therefore, the influence of the measurement noise can be eliminated by setting a relative long sample time. The $\boldsymbol{O}_r$ matrix can be calculated by applying singular value decomposition to Eq. (41). Then according to the first column of $\boldsymbol{O}_r$ matrix in Eq. (33), the $\boldsymbol{C}$ matrix can be determined immediately. The rest columns of $\boldsymbol{O}_r$ matrix can be used to build a matrix equation which describes the relationship between $\boldsymbol{A}$ and $\boldsymbol{C}$ matrix. Therefore, the $\boldsymbol{A}$ matrix can be solved according to the matrix equation by applying a least square method. Finally, the $\boldsymbol{B}$ and $\boldsymbol{D}$ matrix can be solved according to Eq. (34). In summary, the basic procedure of subspace identification algorithm can be concluded as follows:

1) Solve Eq. (28) and calculate $\boldsymbol{Y}$, $\boldsymbol{X}$ and $\boldsymbol{U}$ matrix according to Eq. (30), Eq. (31) and Eq. (36) ~ Eq. (38);

2) Calculate Π_u according to Eq. (40);

3) Solve $\boldsymbol{O}_r$ by applying singular value decomposition to Eq. (41);

4) Solve $\boldsymbol{C}$ matrix according to Eq. (33);

5) Solve $\boldsymbol{A}$ matrix by applying least square method to Eq. (33);

6) Solve $\boldsymbol{B}$ and $\boldsymbol{D}$ matrix by applying least square method to Eq. (34).

5. SET-MEMBERSHIP IDENTIFICATION

The subspace identification can improve the numeric stability of identification. However, if the model structure is complicated and the numbers of parameters to be identified are large, it will bring problems in matrix decomposing. Therefore, the subspace method is only applied to the UAVs which have simple model structures. In order to expand the application area of new techniques to all kinds of rotorcraft, a more powerful identification method based on set-membership identification theory is developed.

5.1. Identification Model

Currently, the set-membership identification method is only used in time domain, so the identification model is chosen to be a rigid body model as Eq. (1) for a manned helicopter or a high order model the same as the one used in subspace identification for UAVs.

5.2. Identification Algorithm

The set-membership identification is used to identify the following linear algebraic model:

(42) $\boldsymbol{y} = \boldsymbol{\theta}^{\mathrm{T}} \bullet \boldsymbol{x} + \boldsymbol{\varepsilon}$

where $\boldsymbol{y}$ is the m×1 output vector, $\boldsymbol{x}$ is the n×1 regressive vector, $\boldsymbol{\theta}$ is the n × m matrix of parameters to be identified, $\boldsymbol{\varepsilon}$ is the m×1 bounded noise vector. The bounded noise vector can be expressed as:

(43) $|\boldsymbol{\varepsilon}| \le \boldsymbol{\sigma}$

The set-membership identification does not need to know the detailed information of noise, the only knowledge required about noise is its bound. So this kind of identification theory does not influenced by unknown noise, and it is quite suitable for identifying the flight dynamics model of a rotorcraft that usually has high level of measurement noise.

- Basic Identification Algorithm

The identification algorithm developed in our research is based on Optimal Bounding Ellipsoid (OBE) method which is quite efficient and robust. Since the noise is bounded, a bounding ellipsoid which represents the upper limit of parameter space can be defined as Eq. (44)

(44) $\Theta = \left\{ \boldsymbol{\theta} : \sum_{i=1}^{t} \lambda_i \left\| \boldsymbol{y}_i - \boldsymbol{\theta}^T \bullet \boldsymbol{x}_i \right\|_2^2 \le \sum_{i=1}^{t} \lambda_i \bullet tr(\boldsymbol{\sigma}_i \boldsymbol{\sigma}_i^T) \right\}$,

in which the $tr(\bullet)$ represents the trace of a matrix.

The Eq. (44) can be expanded and rewritten as a standard ellipsoid equation:

(45) $\Theta_t = \left\{ \boldsymbol{\theta} \middle| tr\left[\left(\boldsymbol{\theta} - \boldsymbol{\theta}_t^c\right)^T \bullet \boldsymbol{P}_t^{-1} / \kappa_t \bullet \left(\boldsymbol{\theta} - \boldsymbol{\theta}_t^c\right) \right] \le 1 \right\}$

in which,

(46) $\boldsymbol{\theta}_t^c = \boldsymbol{P}_t \sum_{i=1}^{t} \lambda_i \boldsymbol{x}_i \boldsymbol{y}_i^T$

(47) $\boldsymbol{P}_t^{-1} = \sum_{i=1}^{t} \lambda_i \boldsymbol{x}_i \boldsymbol{x}_i^T$

(48) $\kappa_t = \sum_{i=1}^{t} \lambda_i \bullet tr(\boldsymbol{\sigma}_i \boldsymbol{\sigma}_i^T) - \sum_{i=1}^{t} \lambda_i \bullet tr(\boldsymbol{y}_i \boldsymbol{y}_i^T) + tr(\boldsymbol{\theta}_t^{cT} \bullet \boldsymbol{P}_t^{-1} \bullet \boldsymbol{\theta}_t^c)$

The iterative form of Eq. (46) ~ Eq. (48) is:

(49) $\begin{cases} \boldsymbol{\theta}_t^c = \boldsymbol{\theta}_{t-1}^c + \lambda_t \boldsymbol{P}_t \boldsymbol{x}_t \boldsymbol{e}_t^T \\ \boldsymbol{P}_t = \boldsymbol{P}_{t-1} - \dfrac{\lambda_t \boldsymbol{P}_{t-1} \boldsymbol{x}_t \boldsymbol{x}_t^T \boldsymbol{P}_{t-1}}{1 + \lambda_t \boldsymbol{x}_t^T \boldsymbol{P}_{t-1} \boldsymbol{x}_t} \\ \kappa_t = \kappa_{t-1} + \lambda_t tr(\boldsymbol{\sigma}_t \boldsymbol{\sigma}_t^T) - \dfrac{\lambda_t \bullet tr(\boldsymbol{e}_t \boldsymbol{e}_t^T)}{1 + \lambda_t \boldsymbol{x}_t^T \boldsymbol{P}_{t-1} \boldsymbol{x}_t} \end{cases}$

The weighting coefficient λ_t can be determined by minimizing the volume of the bounding ellipsoid, then a second order algebraic equation as Eq. (50) is obtained. The λ_t will be the largest positive root of Eq. (50) if it existed.

(50) $a_2 \lambda_t^2 + a_1 \lambda_t + a_0 = 0$

in which,

(51) $a_2 = (n-1) \bullet tr(\boldsymbol{\sigma}_t \boldsymbol{\sigma}_t^T) \bullet (\boldsymbol{x}_t^T \boldsymbol{P}_{t-1} \boldsymbol{x}_t)^2$

(52) $a_1 = \left[(2n-1) \bullet tr(\boldsymbol{\sigma}_t \boldsymbol{\sigma}_t^T) + tr(\boldsymbol{e}_t \boldsymbol{e}_t^T) - \kappa_{t-1} \boldsymbol{x}_t^T \boldsymbol{P}_{t-1} \boldsymbol{x}_t \right] \bullet \boldsymbol{x}_t^T \boldsymbol{P}_{t-1} \boldsymbol{x}_t$

(53) $a_0 = n\left[tr(\boldsymbol{\sigma}_t \boldsymbol{\sigma}_t^T) - tr(\boldsymbol{e}_t \boldsymbol{e}_t^T) \right] - \kappa_{t-1} \boldsymbol{x}_t^T \boldsymbol{P}_{t-1} \boldsymbol{x}_t$

Finally, the basic OBE algorithm can be illustrated in Fig. 4 below.

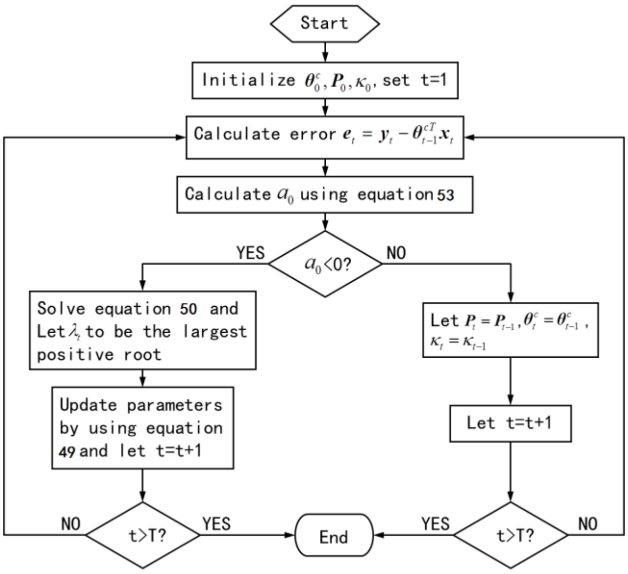

Fig. 4 Basic OBE Algorithm

- Indirect OBE Algorithm for Rotorcraft

The helicopter flight dynamics model is expressed as differential state space equation as shown in Eq. (1), and it is not possible to apply OBE algorithm to identify such model directly. Therefore, an indirect OBE algorithm is derived to satisfy the requirement of identifying a rotorcraft flight dynamics model.

In order to do this, an observation equation as Eq.

(54) is required.

(54) $\boldsymbol{Y} = \boldsymbol{DX} + \boldsymbol{\varepsilon}$

Then based on Taylor series expansion theorem, the Eq. (54) can be transformed to an indirect identification model as shown in Eq. (55).

(55) $\tilde{\boldsymbol{Y}} = \Delta\boldsymbol{\theta}^T \bullet \tilde{\boldsymbol{X}} + \boldsymbol{\varepsilon}$

in which,

(56) $\tilde{\boldsymbol{Y}} = \boldsymbol{Y} - \boldsymbol{DX}(\boldsymbol{\theta}^c)$

(57) $\tilde{\boldsymbol{X}} = \boldsymbol{D}\frac{\partial \boldsymbol{X}}{\partial \boldsymbol{\theta}}\Big|_{\theta=\theta^c}$

(58) $\Delta\boldsymbol{\theta} = \boldsymbol{\theta} - \boldsymbol{\theta}^c$

Finally, the OBE algorithm can be applied to identify the indirect model and then the original parameters can be obtained according to Eq. (58). In summary, the indirect OBE algorithm can be concluded as follows:

1) Set initial value of $\Delta\boldsymbol{\theta}_0$, $\boldsymbol{P}_0$, κ_0 and $\boldsymbol{\theta}_t^c$, let $t=1$;

2) Solve Eq. (1) to get $\boldsymbol{X}(\boldsymbol{\theta}_t^c)$, then $\tilde{\boldsymbol{Y}}$ is obtained;

3) Solve Eq. (9) to get $\frac{\partial \boldsymbol{X}(\boldsymbol{\theta})}{\partial \boldsymbol{\theta}}\Big|_{\theta=\theta_t^c}$, then $\tilde{\boldsymbol{X}}$ is obtained;

4) Use MIMO system OBE algorithm described in Fig. 4 to identify Eq. (55), then the estimation of $\Delta\boldsymbol{\theta}$ is obtained;

5) Let $\boldsymbol{\theta}_{t+1}^c = \boldsymbol{\theta}_t^c + \Delta\boldsymbol{\theta}$ and t=t+1, go to 2.

6. APPICATIONS OF IDENTIFICATION

The developed identification methods are applied to different types of rotorcraft. These applications arise from the requirements of high fidelity models for flying quality analysis, flight control system design of manned helicopters as well as UAVs. In this section, some of these applications will be introduced.

- **Identification for flying quality analysis and flight control system design of a manned helicopter**

The NUAA has worked together with helicopter industries in flying quality design as well as flight control system design research for many years. In order to increase the confidence of the flight dynamics model, the system identification technique is introduced, and a series of flight test for identification purpose has done by a Z-11 research helicopter.

Fig. 5 Z-11 Helicopter

Both rigid body model and high order model with rotor degrees of freedom were identified for different level of flying quality analysis as well as flight control system design. In the early study, the conventional time domain and frequency domain methods were applied, and the set-membership identification technique was used in the last two years to increase the identification accuracy as well as robustness.

Fig. 6 shows the identification results of low order rigid body flight dynamics model. The overall accuracy is good. However, the frequency band of such model is limited which lead to a relative large error in predicting high frequency responses. This kind of model is suitable of basic flying quality analysis and conventional flight control system design.

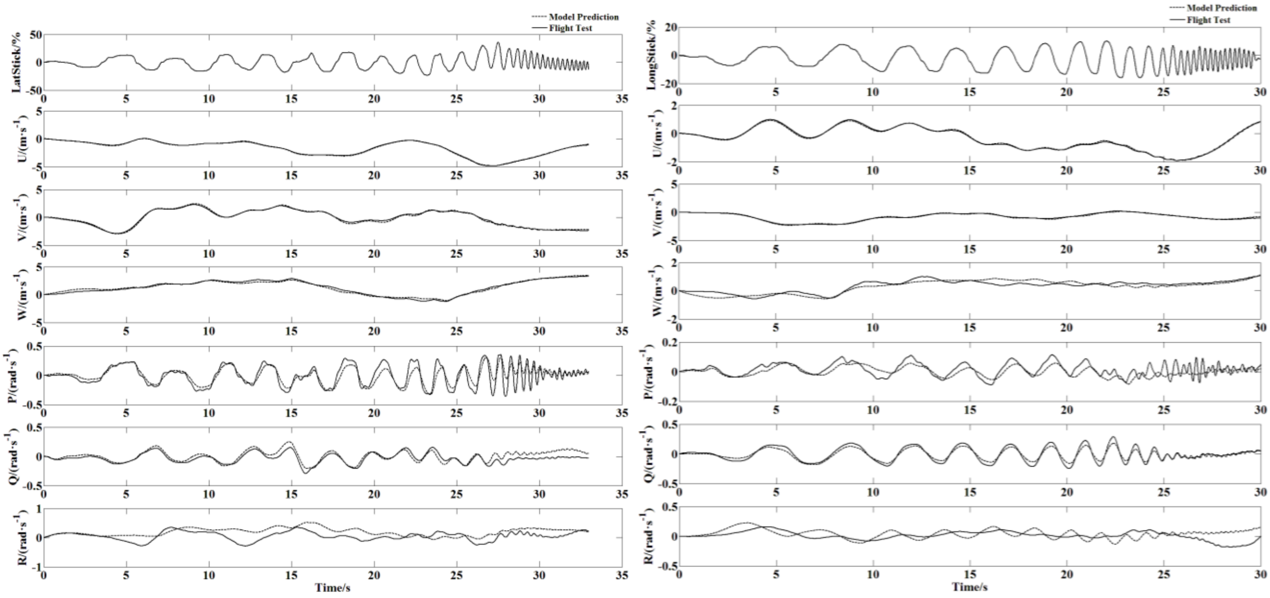

a) b)

Fig. 6 Low Order Model Identification Result

Fig. 7 shows the high order flight dynamics identification results. The introduction of rotor degrees of freedom increases the frequency band of the model. Therefore, the prediction error at high frequency part still remains the same level as low frequency part. Fig. 8 shows the comparison of model accuracy between low order model and high order model. It is obviously that the high order model can follow the high frequency oscillation of response data well. In the contrast, the low order model can only follow the low frequency response. So the high order model can be used to analyse the high level flying quality which considers rigid body mode, rotor mode as well as the rotor-body coupled mode. Another application of such model is the high bandwidth flight control system design.

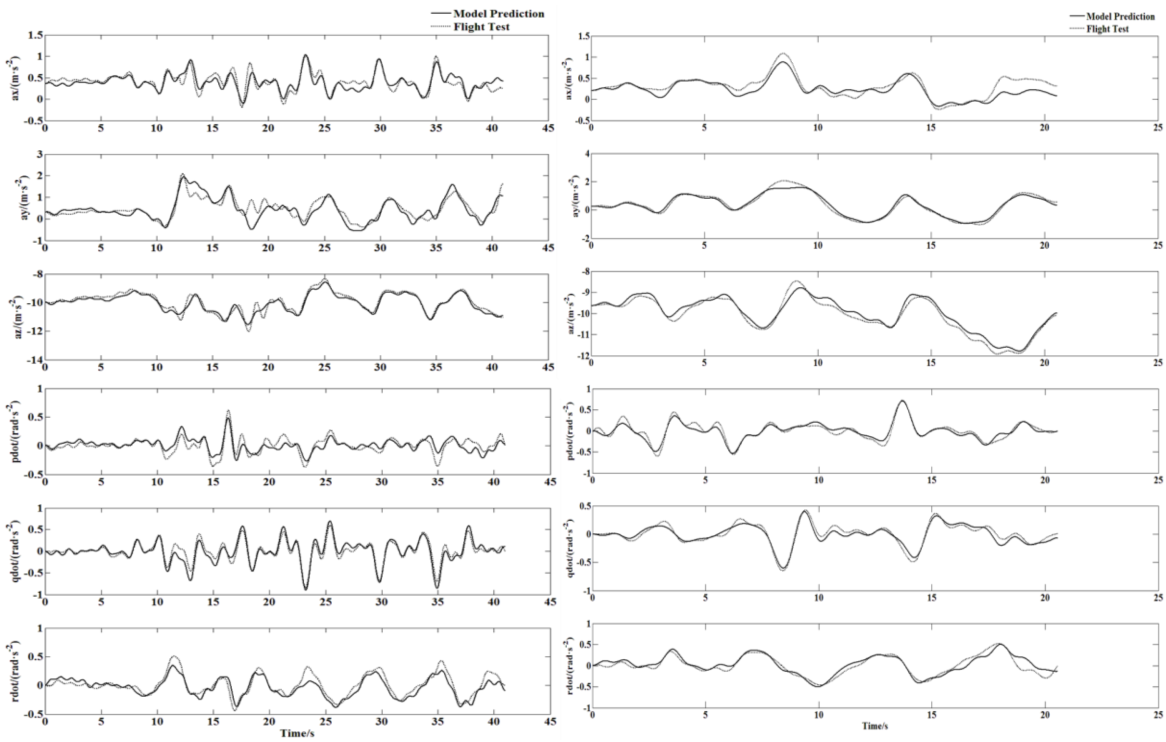

a) b)

Fig. 7 High Order Model Identification Result

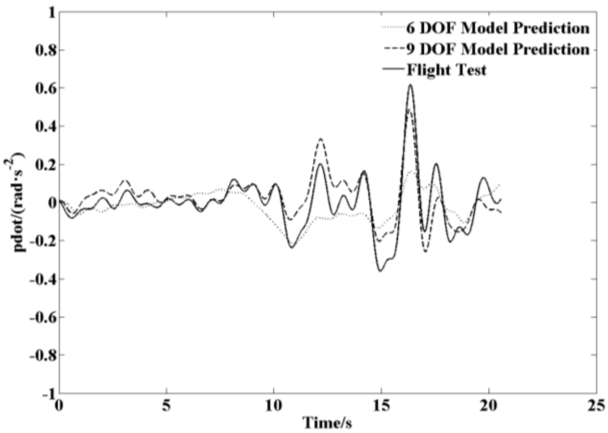

a)

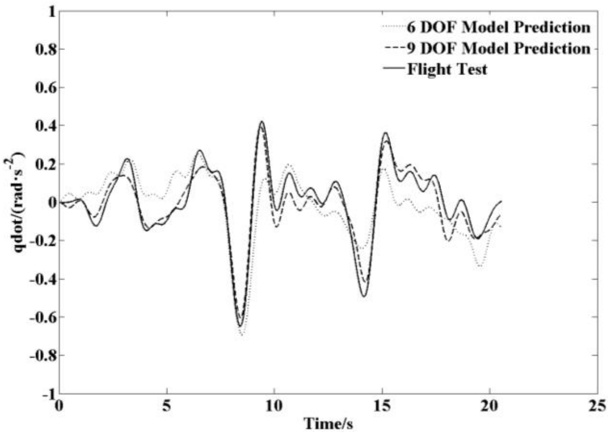

b)

Fig. 8 Comparison of High Order Model with Low Order Model

- **Identification of UAVs**

The unmanned air vehicles have been widely used in many areas. In NUAA, the research on UAV technology has started as early as last century. The system identification technique was used for rapid flight dynamics modeling of several UAVs including helicopters as well as the tilt rotor aircraft. The conventional time domain identification method was applied in early stage, and the subspace identification method has been used to identify the high order model of UAVs since 2008. In recent years, the set-membership identification technique was applied to UAVs for adaptive control system design purpose. All of these identification techniques have provided the accurate flight dynamics models for control system design. It has been proven that the established identification tools can greatly increase the efficiency in the development of UAVs.

Fig. 9 Unmanned Research Helicopter

Fig. 10 Unmanned Tilt Rotor Aircraft

Because the scale of the UAVs is usually small, the response frequency is much higher than the manned helicopters. So the measured data are usually contaminated by high frequency noise heavily. The low signal-to-noise ratio problem brings difficulties in identifying such models with high accuracy. Therefore, the new identification techniques such as subspace identification and especially the set-membership identification that are less influenced by measurement noise have significant advantages.

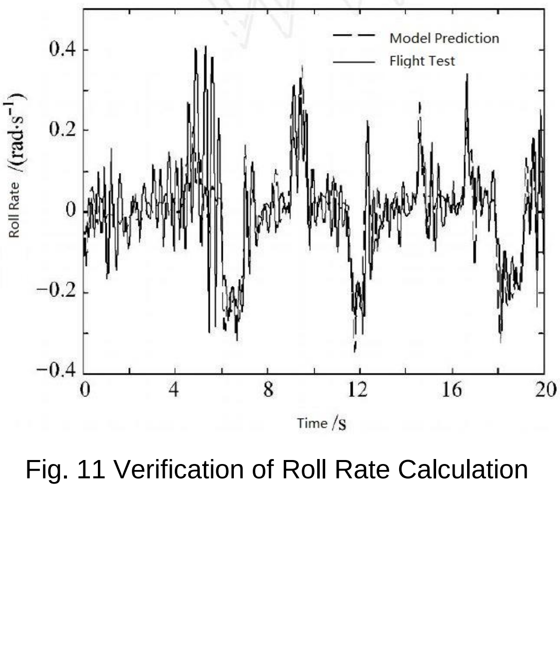

Fig. 11 Verification of Roll Rate Calculation

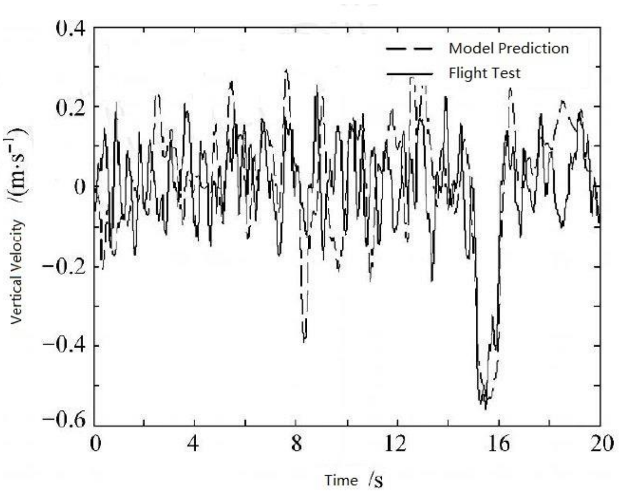

Fig. 12 Verification of Vertical Velocity Calculation

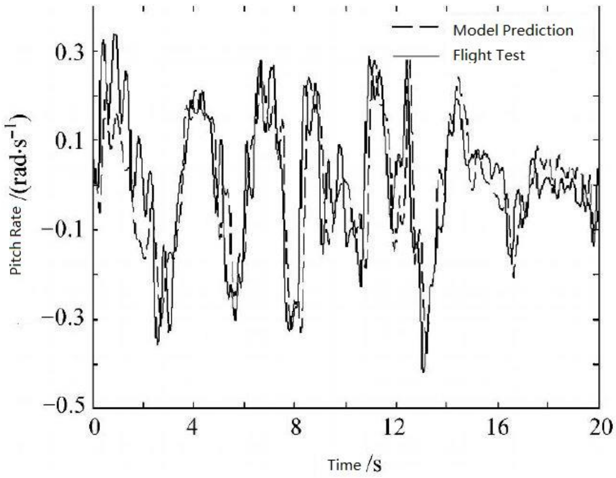

Fig. 13 Verification of Pitch Rate Calculation

The Fig. 14 shows the comparison of set-membership identification with conventional maximum likelihood method. It is obvious that, the new identification technique has better accuracy especially in identifying a model from the test data that have relatively low signal-to-noise ratio.

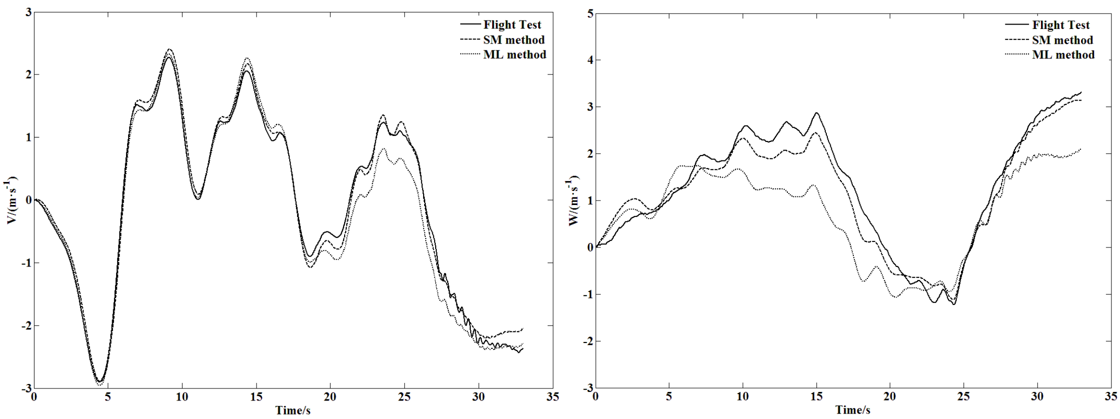

a) b)

Fig. 14 The Comparison of Set-membership Identification with Maximum Likelihood Method

7. CONCLUSIONS

The research on rotorcraft flight dynamics model identification technique as well as its applications in NUAA for the last decade is introduced. The main identification methods are discussed in details. The advantages of the system identification in constructing high fidelity flight dynamics model for flying quality analysis and flight control system design are proven. However, there are still many challenges in rotorcraft system identification technology. For conventional identification methods, the optimal model structure determination is still need to be investigated, and the influence of non-ideal noise should be considered in the parameter identification. For the subspace method, the future research will be focused on eliminating the difficulties in identifying complex models. For set-membership identification, a more comprehensive noise bound determination technique is required and the applications should be expanded to the extended models which contain rotor degrees of freedom in the future.

References

[1] Hamel P. *Rotorcraft system identification*. AGARD-LS-178, 1991.

[2] Eugene A Morelli, Vladislav Klein. Application of system identification to aircraft at NASA Langley

research center. *Journal of Aircraft*, Vol. 42, No. 1, pp 12-25, 2005.

[3] Ravindra Jategaonkar, Dietrich Fischenberg, Wolfgang von Gruenhagen. Aerodynamic modeling and system identification from flight data — recent applications at DLR. *Journal of Aircraft*, Vol. 41, No. 4, pp 681-691, 2004.

[4] Wu Wei, Chen Renliang. Identification method of longitudinal and lateral coupled dynamic model for helicopter. *Journal of Vibration Engineering*, Vol. 22, No. 3, pp 232-236, 2009.

[5] Wu Wei, Chen Renliang. Research on rapid frequency domain identification of helicopter dynamics model in hover. *Journal of Vibration Engineering*, Vol. 23, No. 3, pp 290-297, 2010.

[6] Wu Wei. Identification method for helicopter flight dynamics modeling with rotor degrees of freedom. *Chinese Journal of Aeronautics*, Vol. 27, No. 6, pp 1363-1372, 2014.

[7] Sun Tao, Song Yanguo, Zhang Chenglin. Subspace based system identification of small-scale helicopter flight dynamics. *Journal of Nanjing University of Aeronautics and Astronautics*, Vol. 40, No. 5, pp 589-593, 2008.

[8] Sun Tao, Song Yanguo, Zhang Chenglin. Identification of flight dynamics model of model-scale helicopter in hover condition. *Acta Aeronautica et Astronautica Sinica*, Vol. 30, No. 1, pp 40-45, 2009.

[9] Wu Wei, Chen Renliang. Identification method for helicopter fully coupled flight dynamics model in hover condition. *Acta Aeronautica et Astronautica Sinica*, Vol. 32, No. 2, pp 202-211, 2011.

[10] Wu Wei, Chen Renliang. Set-Membership Identification method for helicopter flight dynamics modeling. *Journal of Aircraft*, Vol. 52, No. 2, pp 553-560, 2015.